S

Structure, Substrate Recognition, and Mechanism of the Na^+-Hydantoin Membrane Transport Protein, Mhp1

Scott M. Jackson[1], Ekaterina Ivanova[2], Antonio N. Calabrese[2], Anna Polyakova[2], David J. Sharples[2], Tatsuro Shimamura[3,4], Florian Brueckner[4,5], Katie J. Simmons[2], Michelle Sahai[6], Homa Majd[6], Edmund Kunji[7], Irshad Ahmad[2], Simone Weyand[4], Shun'ichi Suzuki[8], Alison E. Ashcroft[2], Maria Kokkinidou[9], Arwen Pearson[2,9], Oliver Beckstein[10], Stephen A. Baldwin[2], So Iwata[3,4], Alexander D. Cameron[4,11] and Peter J. F. Henderson[2]

[1]Astbury Centre for Structural Molecular Biology, School of BioMedical Sciences, University of Leeds, Leeds, UK
[2]Astbury Centre for Structural Molecular Biology, Institute of Membrane and Systems Biology, University of Leeds, Leeds, UK
[3]Department of Cell Biology, Graduate School of Medicine, Kyoto University, Kyoto, Japan
[4]Membrane Protein Laboratory, Diamond Light Source, Harwell Science and Innovation Campus, Didcot, UK
[5]Formycon AG, Ludwig-Maximilians Universität München, Munich, Germany
[6]Biomedical Sciences, University of Roehampton, Whitelands College, London, UK
[7]Mitochondrial Biology Unit, University of Cambridge, Cambridge Biomedical Campus, Cambridge, UK
[8]Ajinomoto Co. Inc., Kawasaki, Kanagawa, Japan
[9]Hamburg Centre for Ultrafast Imaging, Universität Hamburg, Hamburg, Germany
[10]Department of Physics, Arizona State University, Tempe, AZ, USA
[11]School of Life Sciences, University of Warwick, Coventry, UK

S. A. Baldwin: deceased.

G. C. K. Roberts, A. Watts (eds.), *Encyclopedia of Biophysics*,
https://doi.org/10.1007/978-3-642-35943-9_10091-1

Synonyms

Ahp1 (originally *Aureobacterium hydantoin* permease); *Arthrobacter aurescens* DSM 3747; HyuP ("permease" in the *hyu* operons from *Pseudomonas* sp. NS671); Mhp1 (*Microbacterium hydantoin* permease); *Microbacterium liquefaciens* AJ 3912 (24); Sodium-hydantoin membrane transport protein, Mhp1

Definition

Mhp1 is a member of the nucleobase cation symporter-1 (NCS-1) family designated A.2.39.5 (Saier et al. 2006, 2009; Ren and Paulsen 2010). The substrates for Mhp1are hydantoins substituted with aromatic groups at the 5-position. The wild-type protein contains 489 amino acids (Suzuki and Henderson 2006), modestly modified in a genetic construct at the N-terminus and C-terminus, where a $(His)_6$ tag is incorporated to facilitate amplified expression, purification, and crystallization (Suzuki and Henderson 2006; Shimamura et al. 2008). The transport reaction of Mhp1 is:

$$\text{Hydantoin (out)} + \text{Na}^+ \text{ (out)} \rightarrow \text{Hydantoin (in)} + \text{Na}^+ \text{ (in)}$$

This reaction is of commercial interest, because of the potential for converting waste hydantoins to compounds of added value, for example, L-amino acids (Suzuki et al. 2005; Javier et al. 2009). Established substrates of Mhp1 are:

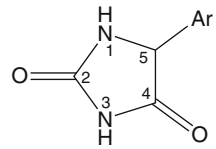

Hydantoin substituted at the 5-position with an aromatic group

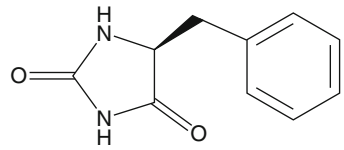

***L*-5-Benzylhydantoin**

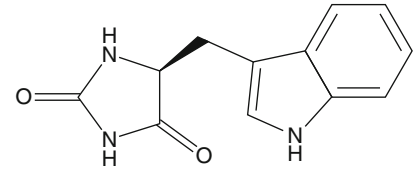

***L*-5-Indolylmethylhydantoin**

Introduction

The first protein of the NCS-1 family to have its structure determined, Mhp1, unexpectedly turned out to be similar in protein fold to the LeuT protein from the neurotransmitter sodium symporter (NSS) family (Yamashita et al. 2005) and the vSGLT sugar sodium symporter (SSS) family (Faham et al. 2008), originally classified as unrelated according to the dissimilarities of their amino acid sequences (Saier et al. 2006). The NCS-1 family is, therefore, part of a subsequently much extended transporter superfamily that has been termed the amino acid-polyamine-organocation (APC) superfamily (Vastermak et al. 2014), the LeuT superfamily, or the five-helix inverted repeat transporter (5HIRT) superfamily (Adelman et al. 2011). The structure of Mhp1 has now been determined in four conformations, including open out, occluded with substrate, occluded with inhibitor, and open in, together with an additional form predicted by molecular dynamics simulations, which illuminate the structural and molecular basis of the alternating access mechanism (Weyand et al. 2008, 2011; Shimamura et al. 2010). The purified Mhp1 protein is sufficiently stable for a range of biophysical and biochemical techniques including crystallization (Shimamura et al. 2008), X-ray diffraction (Weyand et al. 2008; Shimamura et al. 2010; Simmons et al. 2014), chemical modification (Calabrese et al. 2017; Majd et al., unpublished data), mass spectrometry (Calabrese et al. 2017), spectrophotofluorimetry (Weyand et al. 2008), and electron paramagnetic resonance (Kazmier et al. 2014). Additionally, the dynamics of its changes in conformation have been modeled in molecular simulations (e.g., Shimamura et al. 2010; Adelman et al. 2011; Song and Zhu 2015; Sahai, unpublished).

X-Ray Crystal Structure of Mhp1

Helix Packing and Pseudosymmetry

The Mhp1 transporter is comprised of 12 transmembrane helices (Fig. 1). The first ten helices form a structural motif, which is conserved in the LeuT superfamily of proteins (Weyand et al. 2008, 2011; Abramson and Wright 2009; Krishnamurthy et al. 2009; Shimamura et al. 2010). The arrangement consists of helices 1–5 and 6–10, which show an inverted repeat with a twofold axis approximately parallel to the membrane (Fig. 1). The 12 transmembrane helices can be grouped into three segments, which are referred to as the four-helix bundle (transmembrane helices (TM1 and TM2 and their symmetry partners TM6 and TM7) colored red in Fig. 1); the hash motif, which is another four-helix bundle with the appearance of a hash sign ((TM3 and TM4 with TM8 and TM9) colored yellow in Fig. 1); and the C-terminal TM11 and TM12 (colored gray in Fig. 1) (Shimamura et al. 2010; Weyand et al. 2011). The first two motifs are linked by TM5, and the non-membrane helices IN 2–3 and OUT 7–8; TM10 links the hash motif with the C-terminal TM11 and TM12 (Fig. 1). Within helices 5 and 10 (colored blue in Fig. 1), there are significant movements during conformational changes (Fig. 1), so they are also referred to as "flexible helices."

The Na^+ Binding Site

Na^+ is difficult to resolve by X-ray crystallography, its density being similar to that of H_2O. Nevertheless, potential chelating elements (–C=O, –OH) arranged in space in such a way as to present an ideal coordinating site for Na^+ (Weyand et al. 2008, 2011; Shimamura et al. 2010), taken with biochemical evidence of the participation of Na^+ in binding (Weyand et al. 2008, 2011; Jackson et al., unpublished data), is accepted as sufficient identification of a binding site for this cation. By measuring the binding of hydantoin (see below) in the presence of different alkali metal cations, it was deduced that Na^+ is the highly preferred cation $Na^+ >> Li^+ > K^+ > Rb^+$, Cs^+. Furthermore the binding of ligand was unaffected by the concentration of H^+ over the pH range 3–9. The proposed Na^+ binding site in Mhp1 is located at the interface of TM1 and TM8 (Weyand et al. 2008, 2011; Shimamura et al. 2010; Fig. 1). In both the outward-open and outward-occluded structures (Fig. 1), the cation is modeled to interact with the carbonyl oxygen

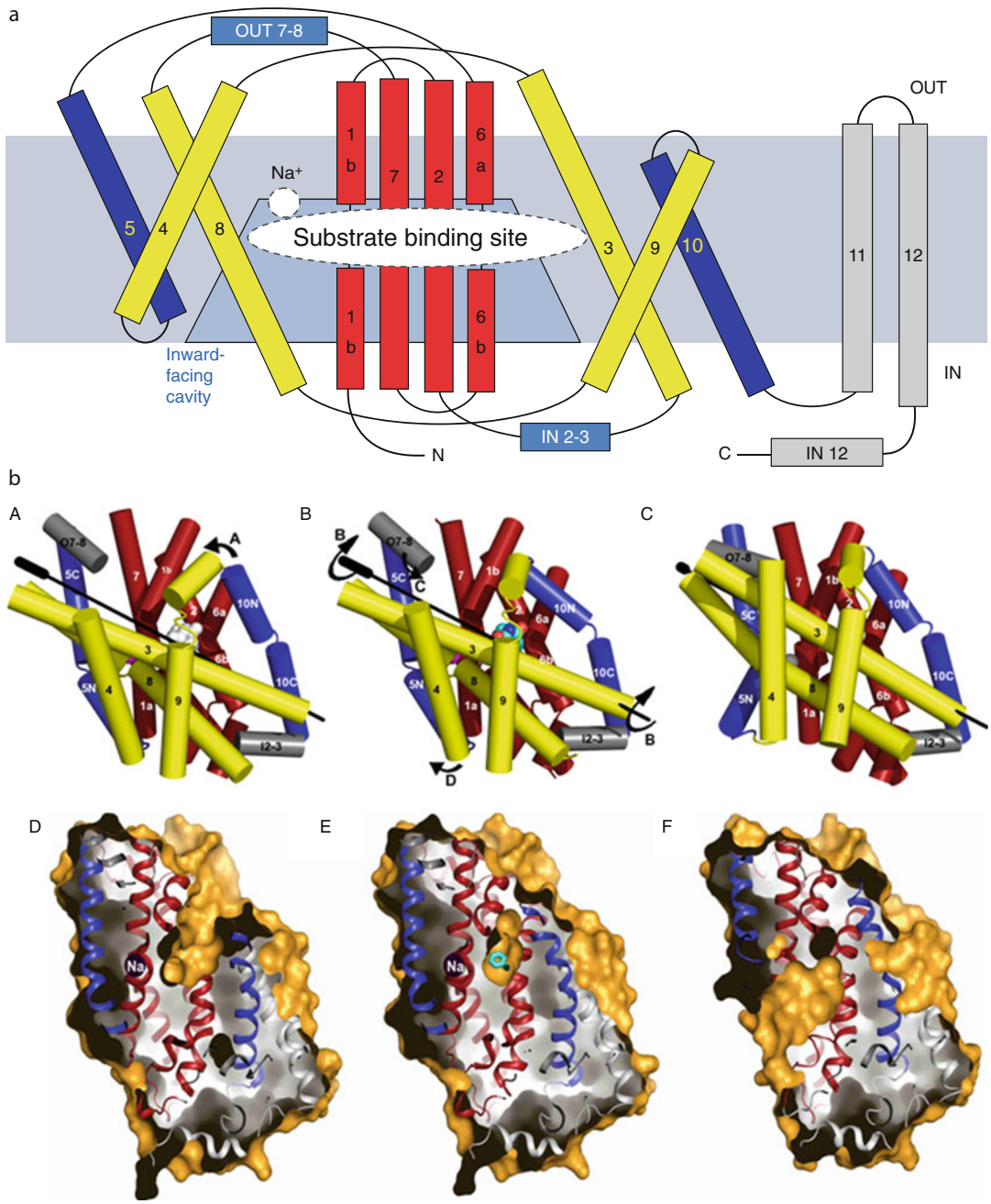

Structure, Substrate Recognition, and Mechanism of the Na^+-Hydantoin Membrane Transport Protein, Mhp1, Fig. 1 Structure of the Mhp1 hydantoin transport protein from *Microbacterium liquefaciens* (**a**) Mhp1 topology. The positions of the substrate and the cation-binding sites are indicated. The membrane is shown in *gray*, and the inward-facing cavity observed in the structure is highlighted in *light blue*. The *horizontal helices* on the "IN" and "OUT" sides of membrane are indicated as "IN" and "OUT." TM3 and TM8 are packed onto each other in three-dimensional space. (**b**) The structures of Mhp1 viewed in the plane of the membrane. *A*, *B*, and *C* show the arrangements of the helices in the outward-open (*A*), closed (*B*), and inward-open (*C*) structures. *D*, *E*, and *F* depict slices through the surface of each of the three structures to reveal the aperture to the outside (*D*), the closed form (*E*) with trapped benzylhydantoin substrate shown in *cyan*, and the aperture to the inside (*F*). The Connolly surface of Mhp1 is shown in *yellow* (calculated with a probe radius of 2 Å). The *ribbon* representation of Mhp1 is shown in *blue* and *red*. (Reproduced by permission of the American

atoms of Ala 38 and Ile 41 in TM1 and of Ala 309 in TM8 and with the –OH groups of Ser 312 and Thr 313 in TM8 (Fig. 2). In the inward-facing structure (Shimamura et al. 2010; Weyand et al. 2011), on the other hand, TM8 has moved ~4.5 Å away from TM1 so that the Na^+ binding site is no longer intact (Fig. 2), reminiscent of the situation in the inward-facing vSGLT and LeuT structures (Faham et al. 2008; Watanabe et al. 2010; Krishnamurthy and Gouaux 2012).

The Substrate Binding Site

The location of the substrate in the Mhp1 molecule was identified in electron density maps of Mhp1 crystals cocrystallized with L-benzylhydantoin, L-indolylmethylhydantoin, bromovinyl hydantoin, and naphthylhydantoin derivatives (Weyand et al. 2008; Simmons et al. 2014; Polyakova et al., unpublished data). An extended electron density was clearly observed at a position almost identical to that of the leucine in the LeuT structure and close to that of the galactose in vSGLT. This site is located at the breaks in the discontinuous TM1 and TM6 and facing TM3 and TM8 (Figs. 1 and 2). It coincides with the foot of the outward-facing cavity (Fig. 1), which is composed of the neighboring surfaces of TM1, TM3, TM6, TM8, and TM10, and allows access of the substrate to the binding site (Fig. 1). An extended structure of L-5-indolylmethylhydantoin determined by small molecule X-ray crystallography was consistent with the shape of this density and with molecular dynamics simulations of the most plausible minimal free energy poses of each of the substrates (Beckstein, unpublished data). The substrate molecules could be modeled between Trp117 (TM3) and Trp220 (TM6) without requiring any modifications of torsion angles (Fig. 2).

The hydantoin moiety forms a pi-stacking interaction with the indole ring of Trp117 and is within hydrogen bonding distance of Asn318 and Gln121 (Simmons et al. 2014; Fig. 3). Trp117 and Asn318 are conserved among all the transporters in the family and Gln121 only varies in the uridine transporter, Fui1 (de Koning and Diallinas 2000). Another conserved residue, Asn314, is within hydrogen bonding distance of Asn318 such that it may hold the asparagine side chain in position to interact with the substrate. The aromatic substituent of the hydantoin moiety is situated next to Trp220 and Gln42 (Figs. 2 and 3). The side chain of Trp220 moves into the binding site with respect to its position in the substrate-free structure (Fig. 2) and forms a pi-stacking interaction with the aromatic moiety (Figs. 2 and 3). In addition the larger substituent groups are progressively more comfortably located in an adjacent hydrophobic region (Figs. 2 and 3; Simmons et al. 2014) such that the affinity decreases naphthylhydantoin > bromovinylhydantoin > indolylhydantoin > benzylhydantoin, as the most effective ligands among over 70 tested (Simmons et al. 2014). These specificities have been confirmed and extended by examining the abilities of these hydantoins to protect cysteine residues against modification by maleimides (Calabrese et al. 2017; Majd et al., unpublished data). Interestingly, allantoin, hydantoin, and tryptophan were not effective ligands. Furthermore, it has become apparent that benzylhydantoin binds to the inward-facing form of Mhp1, though with a lower affinity than it does to the outward-facing form when Na^+ is present (Calabrese et al. 2017); this is compatible with its postulated location in the inward-facing form (Fig. 2).

The Structural Basis of the Alternating Access Mechanism

When interpreting crystallographic and biochemical data for membrane proteins, usually and necessarily, the protein has been studied after solubilization in a compatible detergent. This does not necessarily diminish the validity of the interpretation, but it should be remembered that the natural environment of the protein is a bilayer lipid membrane, and the detergent may have altered the protein's properties.

Structure, Substrate Recognition, and Mechanism of the Na^+-Hydantoin Membrane Transport Protein, Mhp1, Fig. 1 (continued) Association for the Advancement of Science. The programs used to make these and all the structural figures are described in Weyand et al. (2008, 2010, 2011; Shimamura et al. 2010) and their supplementary information)

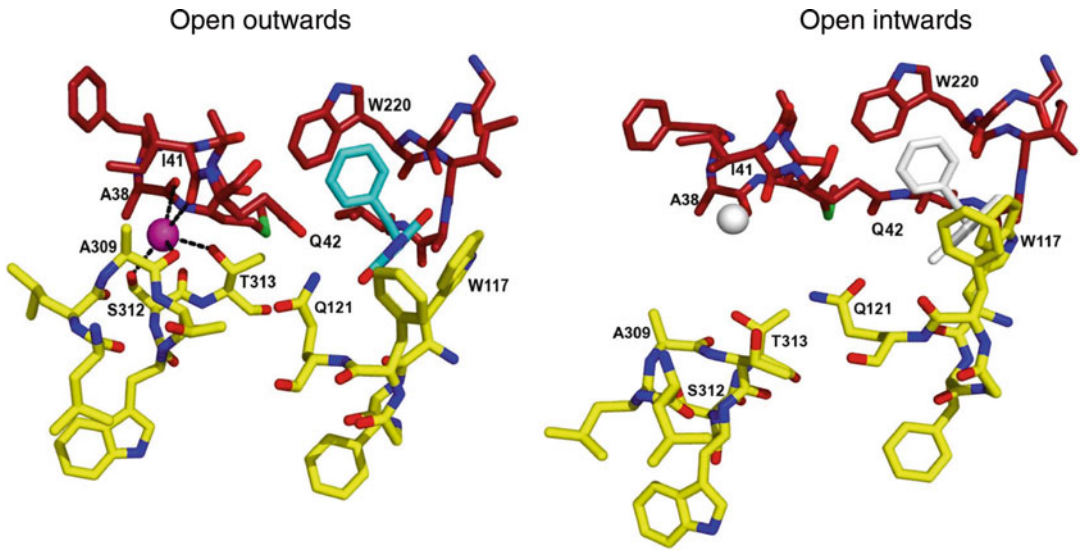

Structure, Substrate Recognition, and Mechanism of the Na^+-Hydantoin Membrane Transport Protein, Mhp1, Fig. 2 The sodium and substrate binding sites in the occluded and inward-open structures taken from Shimamura et al. (2010). The carbon atoms of the amino acids have been colored as in Fig. 1. The sodium ion is represented as a *magenta sphere* and the benzylhydantoin with *cyan* carbon atoms in the occluded structure. In the inward-open structure where these entities are not present, they are represented in *white*

Cys accessibility and quantitative intact mass spectrometry (MS) analyses have recently been devised to study the topological transitions of Mhp1 solubilized in minimal concentrations of dodecylmaltoside (Calabrese et al. 2017). It was found that one natural cysteine residue, Cys327, of the three in Mhp1, has an enhanced solvent accessibility in the inward-facing (relative to the outward-facing) form. Reaction of the purified protein, in detergent, with the thiol-reactive *N*-ethylmaleimide (NEM), resulted in modification of Cys327, suggesting that Mhp1 adopts predominantly inward-facing conformations in the absence of added Na^+ or hydantoin. Addition of either Na^+ ions or the substrate 5-benzyl-L-hydantoin (L-BH) does not change the ratio of inward-facing/outward-facing forms, but systematic co-addition of the two results in an attenuation of labeling, indicating a shift toward outward-facing conformations that can be observed using conventional enzyme kinetic analyses. Such measurements can afford the K_M for each ligand as well as the stoichiometry of about 1 for the Na^+: hydantoin molar binding ratio. Mutations that perturb the Na^+ binding site result either in the protein being unable to adopt outward-facing conformations or in a global destabilization of structure.

The Mhp1 protein has been solved in four different conformational states by X-ray crystallography (Weyand et al. 2008, 2010, 2011; Shimamura et al. 2010) (Fig. 1) including one with an inhibitor bound (Simmons et al. 2014). The outward-facing open and the occluded states show very high similarity, whereas neither of those conformations superimposes well with the inward-facing open state (Fig. 1), leaving the question whether or not there is only one occluded state. Indeed, molecular dynamics simulations suggest the occurrence of an additional inward-facing occluded state (Beckstein, unpublished data; Adelman et al. 2011). The significant movements derived from all known structures appear to be an overall rigid body rotation of the hash motif (helices 3, 4, 8, 9) relative to the bundle (helices 1, 2, 6, 7), which functions in a reciprocating manner around the pseudosymmetrical structural elements of the proteins (cf. Forrest and Rudnick 2009; Boudker and Verdon 2010). The C-terminus (helices 11, 12) moves relatively little in comparison.

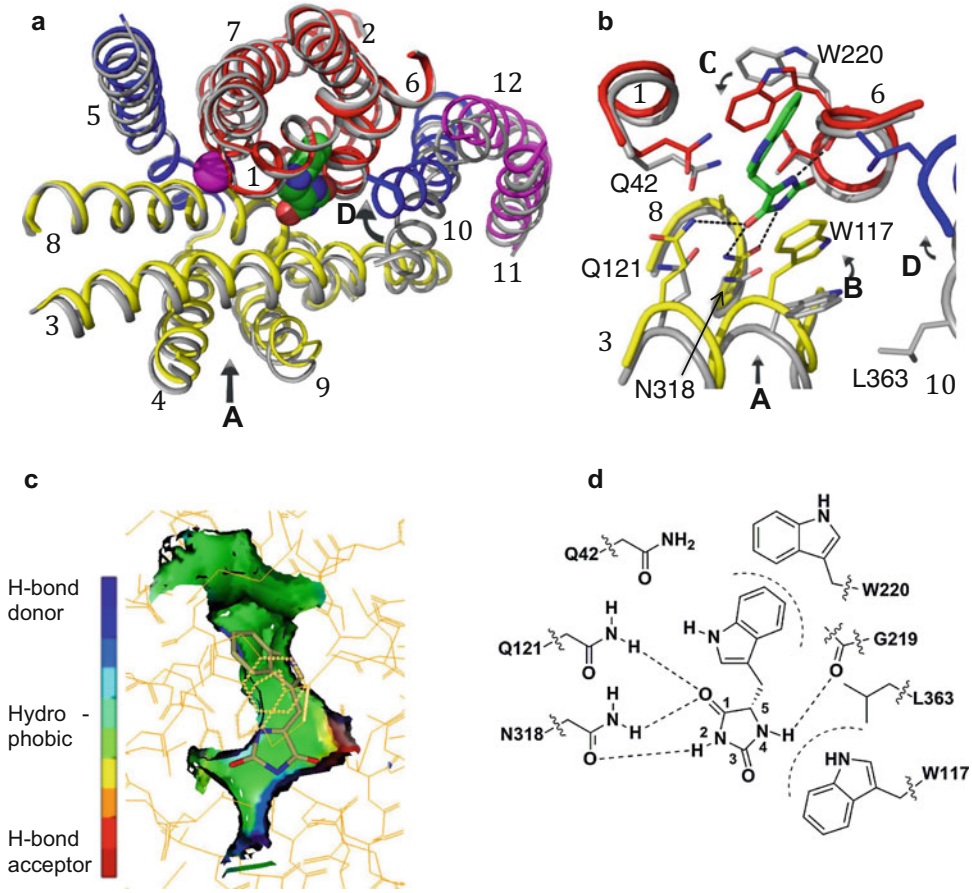

Structure, Substrate Recognition, and Mechanism of the Na^+-Hydantoin Membrane Transport Protein, Mhp1, Fig. 3 Location in Mhp1 protein, hydrophobic milieu, and H-bonding of residues to indolylmethyl-hydantoin in the substrate binding site (**a**) and (**b**) Superposition of the outward-open structure (PDB code 2JLN) onto the IMH-bound structure, optimized using the bundle helices. The IMH structure is shown with the bundle in red, the hash motif in yellow, TM5 and TM10 in blue, and the C-terminal helices in magenta. The outward-open structure is shown in gray. The L-IMH (green spheres) and sodium ion (magenta) bind between the hash and bundle motifs. (**a**) shows an overview of all helices and (**b**) a close-up. The arrows show the main conformational changes that occur upon L-IMH binding. Arrow A: the hash motif rotates toward the bundle with the C-terminal helices partially following. Arrows B and C: Trp117 and Trp220 rotate toward the hydantoin moiety and the 5-indole substituent, respectively, of L-IMH. Arrow D: TM10 flexes and packs over the IMH. (**c**) The extended form of L-IMH in the binding site illustrated using the SPROUT format (Simmons et al. 2014) to show the indole moiety in a hydrophobic pocket (green) (**d**) Schematic of interactions made between L-IMH and the protein. Possible hydrogen bonds are indicated by straight dashed lines and hydrophobic interactions by curved dashed lines

Using the simulation method of dynamic importance sampling, we were able to visualize the functional states of the crystallographic structures of Mhp1 (Fig. 4) and an additional hypothesized conformation in the membrane. The transition between the states can be described as the interplay of a buried thick gate, an external thin gate, and an internal thin gate. The thick gate regulates the conformational change from the outward-facing occluded state to the inward-facing open state and obstructs the ligand binding site toward the intracellular space, when open to the outside. In contrast, the external thin gate comprises only some residues in helix 10, which orchestrate the opening and closing of the outward-facing substrate and Na^+ binding sites.

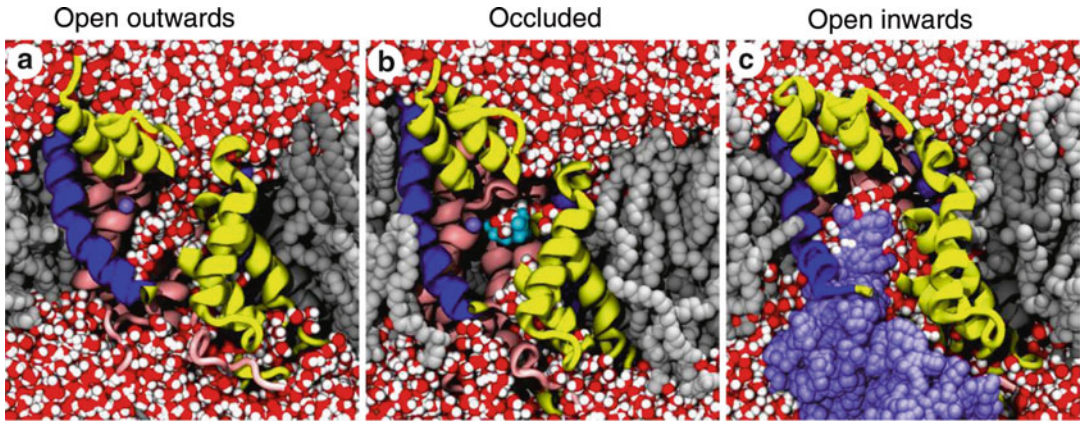

Structure, Substrate Recognition, and Mechanism of the Na^+-Hydantoin Membrane Transport Protein, Mhp1, Fig. 4 Accessibility of the binding sites of Mhp1 in three conformational states. Computer simulations of the Mhp1 transport protein (*helices* in *cartoon* representation, front cut away) in a lipid membrane (*gray*) were carried out to determine the functional states of three crystallographic structures of Mhp1 ((**a**) outward-facing open, 2JLN; (**b**) outward-facing occluded, 2JLO; and (**c**) inward-facing open 2 × 79). Water molecules (*red*/*white*) can only access the substrate and sodium binding site in the open conformations, and the binding sites are sealed in the occluded state. This behavior is predicted by the alternating access mechanism. Repeated simulations showed that the inward-facing conformation (**c**) readily released the bound Na^+ ion; the positions of the ion (*magenta spheres*) from six simulations were all overlaid in *panel c* and define the exit pathway

A complementary region of residues in helix 5 comprises the internal thin gate, which allows opening and release of substrate and Na^+ toward the inside when the external thin gate and thick gates are closed to the outside. The interplay of these events to effect transport is illustrated schematically (Fig. 5). During the conformational changes, the occluded state of the protein always prevents net movement of either cation or substrate without the other – their movement becomes "coupled." Molecular dynamics simulations (Shimamura et al. 2010; Adelman et al. 2011) showed evidence for a sequence of events apparent from the crystallographic structures and fully compatible with the *alternating access mechanism* of transmembrane transport (Jardetzky 1966). This sequence has been extended and modified through the recent implementation of Cys accessibility determination by NEM reactivity, intact MS analysis, peptide mapping, and localization of NEM modification sites to gain insights into the topological states of Mhp1 as follows.

Starting from the stable inward-facing unloaded state of Mhp1, addition of *both* Na^+ and benzylhydantoin substrate altered the equilibrium toward the outward-facing open state (Kazmier et al. 2014; Calabrese et al. 2017). This state binds substituted hydantoin with an affinity greater than that of the inward-facing form. The thin extracellular gate formed by TM10 can then close to form the occluded state with Na^+:hydantoin:Mhp1 in a 1:1:1 ratio. A large conformational change takes place during which the hash motif (the thick gate) swings around an axis roughly parallel to TM3 to form the inward-facing conformation and the external helix moves to close off further the cavity to the external environment. Through subsequent opening of the intracellular thin gate (formed by TM5), the sodium and substrate binding sites become connected to the cytosol, allowing egress of the transported ion and substrate. It is likely that the Na^+ leaves first, since molecular dynamics simulations and structural constraints indicate that dissociation of the ion is extremely fast (Fig. 4), whereas kinetics measurements show that benzylhydantoin can bind appreciably to the inward-facing form (Calabrese et al. 2017).

The structures of LeuT in substrate-free outward-open and apo inward-open states have now been determined (Krishnamurthy and

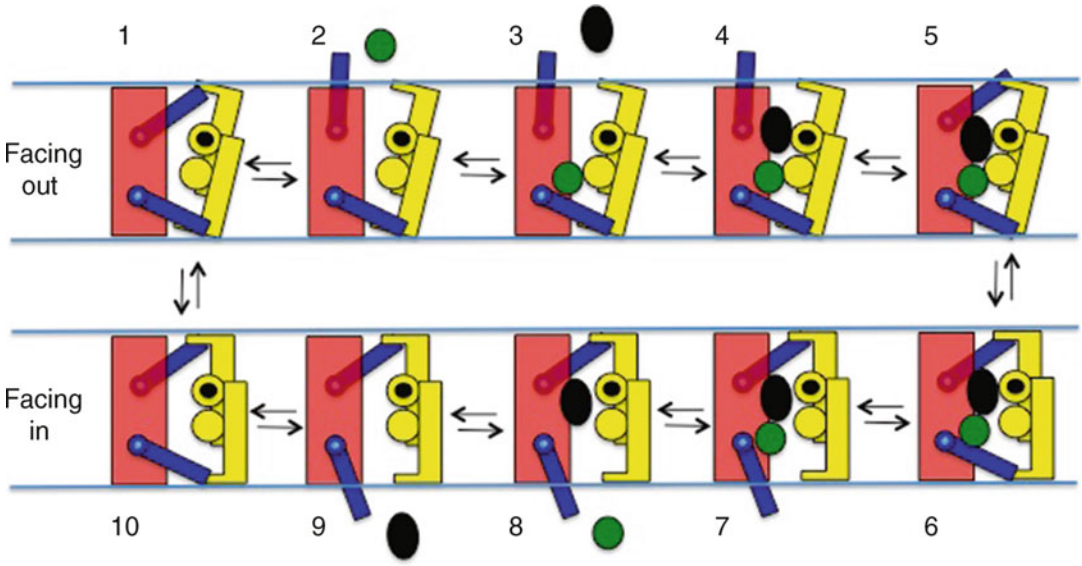

Structure, Substrate Recognition, and Mechanism of the Na^+-Hydantoin Membrane Transport Protein, Mhp1, Fig. 5 Schematic illustration of the possible conformations of an NCS-1 membrane transport protein. The bundle helices *1*, *2*, *6*, *7* are in *red*. The hash motif helices *3*, *4*, *8*, *9* forming the *internal thick gate* are in *yellow*; the *external thin gate* containing part of helix 10 is in *blue*. The *internal thin gate* containing part of helix 5 is also in *blue*. The rotation axis of the *thick gate*, running approximately parallel to TM3, is shown as a *filled black circle* on TM3. The process of transport from outside to inside follows the steps from 1 to 10

Gouaux 2012), adding to the outward-closed form published previously (Yamashita et al. 2005). Its similarities and differences to Mhp1 are discussed by Cameron et al. (2012, Encyclopedia; Kazmier et al. 2013; Claxton et al. 2015).

The Kinetic Features of Alternating Access

While three conformations of Mhp1 have been resolved, the complete process of transport could involve as many as 12 intermediate states (Fig. 5; Forrest et al. 2011). Of course, some of these may be unstable and short-lived and so unlikely to be detected with available biophysical techniques. For example, molecular dynamics simulations suggest the occurrence of an additional conformationally different form of the inward-facing occluded state (Beckstein, unpublished data). Nevertheless, establishing the number of these states and the kinetic constants for their interconversions is the next stage in understanding the molecular mechanism of Mhp1 and defining the differences between members of the NCS-1 family itself and between other members of the 5HIRT superfamily.

Molecular dynamics simulations (Shimamura et al. 2010; Beckstein, unpublished data) suggest that the external and internal gates oscillate rapidly (on the sub-microsecond timescale) and very much faster than hypothesized changes in the conformation of the internal gate or, indeed, observed rates of transport. It is therefore unlikely that any one step involving just a change in the external gates limits the rate of the translocation process. This could simplify the kinetic model (Fig. 5) to a smaller number of relatively stable states.

Measurements of the rates and extents of ligand binding to Mhp1 can be accomplished by following changes in the inherent tryptophan fluorescence of purified Mhp1 (Fig. 6). Binding of a hydantoin is markedly enhanced in the presence of Na^+ ions and shows both a binding step and conformational change (Fig. 6, Ivanova and Jackson, unpublished data). The reciprocal enhancement of Na^+ binding by benzylhydantoin is also

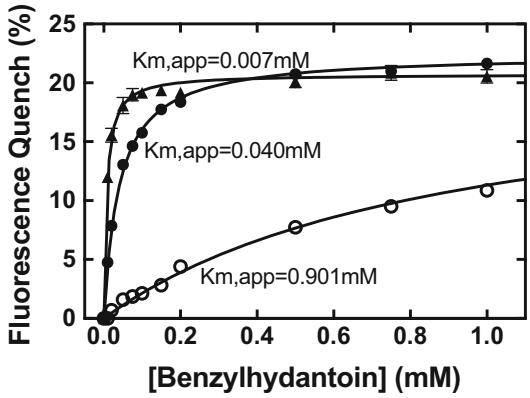

Structure, Substrate Recognition, and Mechanism of the Na^+-Hydantoin Membrane Transport Protein, Mhp1, Fig. 6 Tryptophan fluorescence quenching by L-benzylhydantoin. The Mhp1 solution was titrated by L-benzylhydantoin and/or NaCl and the decrease in the tryptophan fluorescence at 348 nm was monitored. The measurements were performed without added NaCl (*open circles*), with 15 mM NaCl (*closed circles*) and with 140 mM NaCl (*triangles*) in the buffered solution in which compensating concentrations of choline chloride were present to maintain the same ionic composition of 140 mM. The B_{max} values were not significantly different for each dataset – 21.5%, 22.5%, and 20.7%, respectively (For details, see Weyand et al. (2008))

apparent (Fig. 5) – the binding of cation and substrate is coupled. The kinetics of these changes can be profoundly altered by mutating some of the key residues identified above (Jackson and Ivanova, unpublished data).

Summary

The structures of the Na^+-hydantoin transport protein, Mhp1, in outward-open, occluded, and inward-open conformations are summarized. A working model of the alternating access mechanism of transport is derived from detailed examination of the ligand binding sites in the different conformations allied with Cys accessibility studies, kinetic analyses of ligand binding, and molecular dynamics simulations.

Our working model for secondary transport in Mhp1 contains the following steps:

1. At equilibrium and in the absence of substrate and ions, the protein switches spontaneously between the inward-facing and the outward-facing unloaded state, but the inward-facing form predominates.
2. Once Na^+ binds to the outward-facing state, it stabilizes it and promotes the binding of substrate in a 1:1 ratio with its hydantoin moiety in H-bonding configurations with Asn318, Gln121, and Gly219 and with its pi orbitals close to those of Trp117. Additionally the 5′ aromatic substituent fits into a hydrophobic pocket formed partially by the side chain of Trp220.
3. The extracellular thin gate closes.
4. The thick gate switches from outward facing to inward facing, and the external surface helix further closes the prior outward-facing cavity.
5. The intracellular thin gate opens and substrates are released, probably Na^+ first, to the intracellular space.
6. The unloaded protein is now in the stable inward-facing conformation, ready for a repetition of the cycle.

The structure of Mhp1, which is found in a bacterium *Microbacterium liquefaciens*, is used as a paradigm for models of homologous transport proteins found in fungi (e.g., Krypotou et al. 2012, 2015a, b; Sanguinetti et al. 2014) and plants (e.g., Mourad et al. 2012; Schein et al. 2013; Witz et al. 2014; Girke et al. 2014; Rapp et al. 2016). It is likely that the cycle of kinetic events postulated here for Mhp1will also be of use in studies of similar proteins in eukaryotes as well as prokaryotes.

Cross-References

- ▶ Membrane Transport Proteins: The Five-Helix Inverted Repeat Superfamily
- ▶ Membrane Transport, Energetics and Overview
- ▶ Nucleobase-Ascorbate-Transporter (NAT) Family
- ▶ Nucleobase-Cation-Symport-1 Family of Membrane Transport Proteins

- ▶ Structural Aspects of UapA, the H^+-xanthine/Uric Acid Transporter from *Aspergillus nidulans*
- ▶ Uracil: Proton Symporter, UraA

References

Abramson J, Wright EM (2009) Structure and function of Na^+-symporters with inverted repeats. Curr Opin Struct Biol 19:425–432

Adelman JL, Dale AL, Zwier MC, Bhatt D, Chong LT, Zuckerman DM, Grabe M (2011) Simulations of the alternating access mechanism of the sodium symporter Mhp1. Biophys J 101:2399–2407

Boudker O, Verdon G (2010) Structural perspectives on secondary active transporters. Trends Pharmacol Sci 31:418–426

Calabrese AN, Jackson SM, Jones LN, Beckstein O, Heinkel F, Gsponer J, Sans M, Kokkinidou M, Pearson AR, Radford SE, Ashcroft AE, Henderson PJF (2017) Topological dissection of the membrane transport protein Mhp1 derived from cysteine accessibility and mass spectrometry. Anal Chem 89:8844–8852

Claxton DP, Kazmier K, Mishra S, Mchaourab HS (2015) Navigating membrane protein structure, dynamics, and energy landscapes using spin labeling and EPR spectroscopy. Methods Enzymol 564:349–387

Cameron AD, Beckstein O, Henderson PJF (2012) Membrane transport proteins: the five-helix inverted repeat superfamily. Encyclopaedia of Biophysics (Roberts GK, Watts A eds) 3:1481–1485

de Koning H, Diallinas G (2000) Nucleobase transporters. Mol Membr Biol 17:75–94

Faham S, Watanabe A, Besserer GM, Cascio D, Specht A, Hirayama BA, Wright EM, Abramson J (2008) The crystal structure of a sodium galactose transporter reveals mechanistic insights into Na^+-sugar symport. Science 321:810–814

Forrest LR, Rudnick G (2009) The rocking bundle: a mechanism for ion-coupled solute flux by symmetrical transporters. Physiology 24:377–386

Forrest LR, Kraemer R, Ziegler C (2011) The structural basis of secondary active transport mechanisms. Biochim Biophys Acta 1807:167–188

Girke C, Daumann M, Niopek-Witz S, Mohlmann T (2014) Nucleobase and nucleoside transport and integration into plant metabolism. Front Plant Sci 5:443

Jardetzky O (1966) Simple allosteric model for membrane pumps. Nature 211:969–970

Javier Las Heras-Vázquez F, Clemente-Jiménez JM, Martínez-Rodríguez S, Rodríguez-Vico F (2009) Hydantoin racemase: the key enzyme for the production of optically pure α-amino acids, Chap 12. In: Fessner W-D, Anthonsen T (eds) Modern biocatalysis: stereoselective and environmentally friendly reactions. Wiley-VCH, Weinheim

Kazmier K, Sharma S, Islam SM, Roux B, Mchaourab HS (2014) Conformational cycle and ion coupling mechanism of the Na^+/hydantoin transporter Mhp1. Proc Natl Acad Sci U S A 111:14752–14757

Krishnamurthy H, Gouaux E (2012) X-ray structures of LeuT in substrate-free outward-open and apo inward-open states. Nature 481(7382):469–474

Krishnamurthy H, Piscitelli CL, Gouaux E (2009) Unlocking the molecular secrets of sodium-coupled transporters. Nature 459:347–355

Krypotou E, Kosti V, Amillis S, Myrianthopoulos V, Mikros E, Diallinas G (2012) Modeling, substrate docking, and mutational analysis identify residues essential for the function and specificity of a eukaryotic purine-cytosine NCS1 transporter. J Biol Chem 287(44):36792–36803

Krypotou E, Evangelidis T, Bobonis J, Pittis AA, Gabaldon T, Scazzocchio C, Mikros E, Diallinas G (2015a) Origin, diversification and substrate specificity in the family of NCS1/FUR transporters. Mol Microbiol 96(5):927–950

Krypotou E, Scazzocchio C, Diallinas G (2015b) Functional characterization of NAT/NCS2 proteins of *Aspergillus brasiliensis* reveals a genuine xanthine-uric acid transporter and an intrinsically misfolded polypeptide. Fungal Genet Biol 75:56–63

Mourad GS, Tippmann-Crosby J, Hunt KA, Gicheru Y, Bade K, Mansfield TA, Schultes NP (2012) Genetic and molecular characterization reveals a unique nucleobase cation symporter 1 in Arabidopsis. FEBS Lett 586(9):1370–1378

Rapp M, Schein J, Hunt KA, Nalam V, Mourad GS, Schultes NP (2016) The solute specificity profiles of nucleobase cation symporter 1 (NCS1) from Zea mays and *Setaria viridis* illustrate functional flexibility. Protoplasma 253(2):611–623

Ren Q, Paulsen IT (2010) Transport DB. http://www.membranetransport.org/. Accessed 1 May 2012

Saier MH, Tran CV, Barabote RD (2006) TCDB: the transporter classification database for membrane transport protein analyses and information. Nucleic Acids Res 34(Database issue):D181–D186

Saier MH Jr, Yen MR, Noto K, Tamang DG, Elkan C (2009) The transporter classification database: recent advances. Nucleic Acids Res 37:D274–D278

Sanguinetti M, Amillis S, Pantano S, Scazzocchio C, Ramon A (2014) Modelling and mutational analysis of *Aspergillus nidulans* UreA, a member of the subfamily of urea/H(+) transporters in fungi and plants. Open Biol 4(6):140070

Schein JR, Hunt KA, Minton JA, Schultes NP, Mourad GS (2013) The nucleobase cation symporter 1 of *Chlamydomonas reinhardtii* and that of the evolutionarily distant *Arabidopsis thaliana* display parallel function and establish a plant-specific solute transport profile. Plant Physiol Biochem 70:52–60

Shimamura T, Yajima S, O'Reilly J, Rutherford NG, Henderson PJF, Iwata S (2008) Crystallization of the

hydantoin transporter Mhp1 from *Microbacterium liquefaciens*. Acta Crystallogr F64:1172–1174

Shimamura T, Weyand S, Beckstein O, Rutherford NG, Hadden JM, Sharples D, Sansom MPS, Iwata S, Henderson PJF, Cameron AD (2010) Molecular basis of alternating access membrane transport by the sodium-hydantoin transporter, Mhp1. Science 328:470–473

Simmons KJ, Jackson SM, Brueckner F, Patching SG, Beckstein O, Ivanova E, Geng T, Weyand S, Drew D, Lanigan J, Sharples DJ, Sansom MS, Iwata S, Fishwick CW, Johnson AP, Cameron AD, Henderson PJ (2014) Molecular mechanism of ligand recognition by membrane transport protein, Mhp1. EMBO J 33:1831–1844

Song HD, Zhu F (2015) Conformational changes in two inter-helical loops of Mhp1 membrane transporter. PLoS One 10(7):e0133388

Suzuki S, Henderson PJF (2006) The hydantoin transport protein from *Microbacterium liquefaciens*. J Bacteriol 188:3329–3336

Suzuki S, Takenaka Y, Onishi N, Yokozeki K (2005) Molecular cloning and expression of the *hyu* genes of *Microbacterium liquefaciens* responsible for the conversion of 5-substituted hydantoins to alpha amino acids, in *Escherichia coli*. Biosci Biotechnol Biochem 69:1473–1482

Vastermak A, Wollwage S, Houle ME, Rio R, Saier MH Jr (2014) Expansion of the APC superfamily of secondary carriers. Proteins 82:2797–2811

Watanabe A, Choe S, Chaptal V, Rosenberg JM, Wright EM, Grabe M, Abramson J (2010) The mechanism of sodium and substrate release from the binding pocket of vSGLT. Nature 468:988–991

Weyand S, Shimamura T, Yajima S, Suzuki S, Mirza O, Krusong K, Carpenter EP, Rutherford NG, Hadden JM, O'Reilly J, Ma P, Saidijam M, Patching SG, Hope RJ, Norbertczak HT, Roach PCJ, Iwata S, Henderson PJF, Cameron AD (2008) Molecular basis of the alternating access model of membrane transport: structure of a nucleobase-cation-symport-1 family transporter. Science 322:709–713

Weyand S, Ma P, Beckstein O, Baldwin J, Jackson S, Suzuki S, Shimamura T, Sansom MSP, Iwata S, Cameron AD, Baldwin SA, Henderson PJF (2010) The nucleobase-cation-symport-1 family of membrane transport proteins. In: Messerschmidt A (ed) Handbook of metalloproteins. Wiley, Chichester, pp 848–864

Weyand S, Shimamura T, Beckstein O, Sansom MPS, Iwata S, Henderson PJF, Cameron AD (2011) The alternating access mechanism of transport as observed in the sodium-hydantoin transporter Mhp1. J Synchrotron Radiat 18:20–23

Witz S, Panwar P, Schober M, Deppe J, Pasha FA, Lemieux MJ, Mohlmann T (2014) Structure-function relationship of a plant NCS1 member – homology modeling and mutagenesis identified residues critical for substrate specificity of PLUTO, a nucleobase transporter from Arabidopsis. PLoS One 9(3):pe91343

Yamashita A, Singh SK, Kawate T, Jin Y, Gouaux E (2005) Crystal structure of a bacterial homologue of Na^+/Cl^--dependent neurotransmitter transporters. Nature 437: 215–223